Joint Conference of ISR 2006 - 37th International Symposium on Robotics - and ROBOTIK 2006 - 4th German Conference on Robotics, 15-18 May 2006, Munich, Germany, Session C5.

A MULTI-MODEL SET MEMBERSHIP ESTIMATOR FOR MOBILE ROBOT LOCALIZATION

Sylvia Horn
Technische Universität Dresden
Germany

Klaus Janschek
Technische Universität Dresden
Germany

Speaker: **Sylvia Horn, Technische Universität Dresden, Germany**
sylvia.horn@tu-dresden.de

Topic: **C5 – Mobile Robot Localization**
Keywords: **set theoretic estimation, ellipsoid set, parallelepiped set, data fusion, localization**

Abstract – This paper covers the problem of state estimation with uncertainty descriptions by convex sets. It is known that existing estimation schemes using compact convex geometrical structures such as boxes, ellipsoids or parallelepipeds are suffering from considerable over-approximations depending on the system structure and maybe inconvenient operational conditions. Solving this problem the current paper introduces a novel multi – model set membership estimator, which combines the strengths of the named different set theoretic descriptions to get minimum volume uncertainty regions. This concept is implemented in a two stage fusion scheme using unified set based fusion algorithms: (a) propagation fusion, where competing prediction estimates are fused for minimum uncertainty region and (b) measurement fusion, where the minimum uncertainty prediction estimate is fused with uncertain measurements. By using these fusion techniques and with the assumption that the true state is part of the initial set the novel filter reaches a robust estimation of the required system states.
The paper recalls the basic principles of set theoretic descriptions using boxes, ellipsoids and parallelepipeds. It introduces the concept, the detailed structure and the fusion scheme of the multi-model set membership estimator. The potentials of the proposed estimator are shown by its application to the problem of localization for a differential-drive mobile robot in a flat environment and proved by simulation results.

1. Introduction

In many technical systems the internal states, which are for instance required for control or navigation purposes, are not directly observable and have to be estimated on the basis of uncertain measurements of the system output. Common approaches are based on stochastic descriptions of the uncertainties and employ (extended or unscented) Kalman filtering techniques using (non)linear system and measurement models. In the special case of mobile robot localization the Extended Kalman Filter for example is used for comparing sensor signals and environment descriptions (Cox, 1991; Leonard and Durrant-Whyte, 1991) or for localization via map matching (Thrun, 1993). This approach requires always an exact knowledge of the existing uncertainties distribution.
A more general approach in handling uncertainties is based on set membership or set theoretic methods which use geometrical properties of uncertainties that are unknown from their internal structure but known to be bounded. The uncertainty regions can be described by compact convex geometrical structures such as boxes (Alefeld and Herzberger, 1983), ellipsoids (Schweppe, 1968; Ros et al., 2002) or parallelepipeds – also called parallelotops – (Lohner, 1988; Vicino and Zappa, 1996). Going back to the question of mobile robotics - the named set theoretic algorithms have already been used for bundle of problems. Interval set descriptions come always into operation, when instead of exact parameters only their upper and lower limits are known. Parallelepiped sets have been used e.g. by (Di Marco et al., 2003) for developing a simultaneous localization and map building algorithm for a team of cooperating robots, or by (Garulli and Vicino, 2001) for a localization algorithm via angle measurements. Applications using the ellipsoid set description can be found in (Hanebeck and Schmidt, 1997) or (Hanebeck and Horn, 2000).
It is evident that depending on the system structure and the specific operational conditions the different approaches result in more or less conservative over-approximations of the true uncertainty sets. Solving this problem the current paper introduces a novel multi – model set membership estimator, which combines the strengths of the named different set theoretic descriptions to get minimum volume uncertainty regions. This idea is implemented in a two stage fusion scheme using unified set based fusion algorithms: (a) propagation fusion, where competing prediction estimates are fused for minimum uncertainty region and (b) measurement fusion, where the optimal prediction estimate is fused with uncertain measurements. The potentials of the proposed estimator are shown by its application to the problem of localization for a differential-drive mobile robot in a flat environment. This paper reports on performance evaluation results based on

detailed simulation studies. An extended version of the estimator is currently being implemented on a mobile robot platform and its testing is in progress.

This paper is organized as follows. Section 2 gives a brief introduction to the problem formulation. Section 3 summarizes the three different kinds of set theoretic description used for the implemented multi-model set membership estimator and gives some of the basic mathematic formulas (see (Horn, 2003) for more detailed explanations). A description of the composition of the multi-model set membership estimator can be found in section 4. The following section 5 introduces the exemplary mobile robot platform, which was used to evaluate the developed algorithms and reports the results of the executed simulations. Concluding remarks are given in Section 6.

2. The estimation problem

The problem to be solved is to determine the states of a n-dimensional nonlinear time-discrete system

$$\mathbf{x}_k = f\left(\mathbf{x}_{k-1}, \mathbf{u}_k\right) \tag{1}$$

with the output measurement equation

$$\mathbf{x}_k^M = g\left(\mathbf{x}_k\right) + \mathbf{v}_k . \tag{2}$$

and the input measurement equation

$$\mathbf{u}_k^M = \mathbf{u}_k + \mathbf{w}_k . \tag{3}$$

Here $\mathbf{x}_k$ refers to the *n*-dimensional state space vector at time step k, the *m*-dimensional vector $\mathbf{x}_k^M$ marks the accomplished observations at k, $\mathbf{u}_k$ refers to the *p*-dimensional unknown but measurable system input at k and $\mathbf{u}_k^M$ marks the *p*-dimensional input measurements (e.g. for a mobile robot kinematic system model some odometry, angular increments, etc. will be available). Further it is considered that the input and output measurements of system (1) is corrupted by an additive input measurement uncertainty $\mathbf{w}_k \in \mathbb{R}^p$ and an additive output measurement uncertainty $\mathbf{v}_k \in \mathbb{R}^m$.

The underlying properties of $\mathbf{w}_k$ and $\mathbf{v}_k$ can be assumed to be unknown but they are considered to be bounded by the sets:

$$\underline{\mathbf{e}}_i = \left[\mathbf{e}_i^-, \mathbf{e}_i^+\right], \quad i \in \{w, v\} . \tag{4}$$

Here $\underline{\mathbf{e}}_i$ denotes an interval vector with a lower bound $\mathbf{e}_i^-$ and an upper bound $\mathbf{e}_i^+$. This appears in case of geometric tolerances, quantization problems, bounded noise sources or less examined sensor systems.

To apply the multi-model set membership estimation filter for calculating the estimated states $\hat{\mathbf{x}}_k$ a linear, time-variant filter state space model can be derived by linearization of the system equation (1) and by using the measured input (3)

$$\hat{\mathbf{x}}_k = \mathbf{A}_k \hat{\mathbf{x}}_{k-1} + \mathbf{B}_k \left(\mathbf{u}_k + \mathbf{w}_k\right) \tag{5}$$

with the time variant state matrix $\mathbf{A}_k \in \mathbb{R}^{n \times n}$ and the time variant input matrix $\mathbf{B}_k \in \mathbb{R}^{n \times p}$.

The intention of this paper is to present a multi-model set membership estimation filter that gives estimates $\hat{\mathbf{x}}$ of the true states $\mathbf{x}$ of the system (1) at every time step and without knowing the exact uncertainties except their bounds.

3. Set theoretic description

Interval set description. The interval (box) set

$$\mathcal{X}^{\square} := \underline{\mathbf{x}}^{\square} = \left[\mathbf{x}^-, \mathbf{x}^+\right]$$

is defined by the *n*-dimensional interval vector $\underline{\mathbf{x}}^{\square}$. The Volume $V^{\square}$ of $\mathcal{X}^{\square}$ can be easily computed as

$$V^{\square}\left(\mathcal{X}^{\square}\right) := \prod_{i=1}^{n} \left|x_i^+ - x_i^-\right|$$

where x_i^* refers to the *i*th element of the vector $\mathbf{x}^*$ respectively.

Furthermore

$$\mathcal{X}^{S_{\square}} = \left[\max\left({}^1\mathbf{x}^-, {}^2\mathbf{x}^-\right), \min\left({}^1\mathbf{x}^+, {}^2\mathbf{x}^+\right)\right]$$

calculates the intersection between two given intersecting interval sets ${}^1\mathcal{X}^{\square}$ and ${}^2\mathcal{X}^{\square}$.

Ellipsoid set description. A real n-dimensional ellipsoid, centred on $\breve{\mathbf{x}}$, can be concisely described as

$$\mathcal{X}^{\bigcirc} := \left\{ \mathbf{x}^{\bigcirc} : \left(\mathbf{x}^{\bigcirc} - \breve{\mathbf{x}} \right)^{T} \mathbf{X} \left(\mathbf{x}^{\bigcirc} - \breve{\mathbf{x}} \right) \leq 1 \right\}$$

where $\mathbf{X}$ is a positive-semidefinite symmetric $n \times n$ matrix. Considering V_n being the Volume of the unit ball in $\mathbb{R}^n$ the Volume of $\mathcal{X}^{\bigcirc}$ is given by

$$V^{\bigcirc}\left(\mathcal{X}^{\bigcirc}\right) = \frac{V_n}{\sqrt{\det\left(\mathbf{X}\right)}}.$$

A family of ellipsoids which wrap the intersection of ${}^{1}\mathcal{X}^{\bigcirc}$ and ${}^{2}\mathcal{X}^{\bigcirc}$ can be described through

$$\mathcal{X}^{S_{\bigcirc}} = \left\{ \mathbf{x}^{\bigcirc} : \left(0.5 - \lambda\right)\left(\mathbf{x}^{\bigcirc} - {}^{1}\breve{\mathbf{x}} \right)^{T} {}^{1}\mathbf{X} \left(\mathbf{x}^{\bigcirc} - {}^{1}\breve{\mathbf{x}} \right) + \left(0.5 + \lambda\right)\left(\mathbf{x}^{\bigcirc} - {}^{2}\breve{\mathbf{x}} \right)^{T} {}^{2}\mathbf{X} \left(\mathbf{x}^{\bigcirc} - {}^{2}\breve{\mathbf{x}} \right) \leq 1 \right\}$$

with $\lambda \in \left[-0.5, 0.5\right]$. To receive a tight circumscription λ should be chosen that $V^{\bigcirc}\left(\mathcal{X}^{S_{\bigcirc}}\right)$ is minimized. Different methods for calculating λ can be found in (Hanebeck, 1996) or (Ros et al., 2002).

Parallelepiped (parallelotop) set description. A parallelepiped

$$\mathcal{X}^{\Diamond} := \mathbf{T} \Diamond \underline{\mathbf{x}}^{\Diamond}$$

is given by the regular $n \times n$ matrix $\mathbf{T}$ and the n-dimensional interval vector $\underline{\mathbf{x}}^{\Diamond}$. Here the operation sign $\Diamond$ refers to a special kind of matrix-vector multiplication: $n-1$ vertices of $\underline{\mathbf{x}}^{\Diamond}$ will be multiplied with $\mathbf{T}$. The volume of $\mathcal{X}^{\Diamond}$ can be calculated as

$$V^{\Diamond} = \left|\det \mathbf{T}\right| V^{\square}\left(\underline{\mathbf{x}}^{\Diamond}\right)$$

The parallelepiped which circumscribes the intersection of ${}^{1}\mathcal{X}^{\Diamond}$ and ${}^{2}\mathcal{X}^{\Diamond}$ can be geometrically formed via translational displacement of the edges of the parallelepipeds. Mathematically this can be characterized by

$${}^{1}\mathcal{X}^{S_{\Diamond}} = {}^{1}\mathbf{T} \Diamond \left({}^{1}\underline{\mathbf{x}}^{\Diamond} \cap \left({}^{1}\mathbf{T}\right)^{-1} {}^{2}\mathbf{T} \;\; {}^{2}\underline{\mathbf{x}}^{\Diamond} \right) \tag{6}$$

and

$${}^{2}\mathcal{X}^{S_{\Diamond}} = {}^{2}\mathbf{T} \Diamond \left({}^{2}\underline{\mathbf{x}}^{\Diamond} \cap \left({}^{2}\mathbf{T}\right)^{-1} {}^{1}\mathbf{T} \;\; {}^{1}\underline{\mathbf{x}}^{\Diamond} \right) \tag{7}$$

respectively. As above - in order to generate a tight circumscribing set - the parallelepiped (6) or (7) with the smallest volume is chosen.

4. The Multi-Model Estimation Concept

The aim of the introduced multi-model set membership estimator is to combine the strengths of the different set theoretic descriptions to gain a more tight uncertainty region and thus less conservative over-approximations (see Figure 1). The estimator is functionally split into two stages.

In the first stage – the propagation stage or prediction step of the estimator - a new predicted state estimate $\hat{\mathbf{x}}_k$ starting from the present state $\hat{\mathbf{x}}_{k-1}$ and the measured system input $\mathbf{u}_k^M$ is propagated for each of the mentioned set theoretic techniques as indicated with $\mathcal{X}_{k-1}^{i} \rightarrow \mathcal{X}_{k}^{i} \quad i \in \left\{\square, \Diamond, \bigcirc\right\}$ in the block diagram. A subsequent propagation fusion computes for the intersection

$$\mathcal{X}_{k}^{S} = \mathcal{X}_{k}^{\square} \cap \mathcal{X}_{k}^{\bigcirc} \cap \mathcal{X}_{k}^{\Diamond} \tag{8}$$

the minimum volume circumscription

$$\mathcal{X}^{S*} = \min Volume\left(\mathcal{X}^{*}\left(\mathcal{X}^{S}\right)\right), \quad * \in \left\{\square, \Diamond, \bigcirc\right\} \tag{9}$$

of the different model outputs, where $\mathcal{X}^{*}\left(\mathcal{X}^{S}\right)$ means a circumscription of $\mathcal{X}^{S}$ with the convex set $\mathcal{X}^{*}$. This fusion task can be solved by using numerical procedures or with the help of the analytic methods introduced later on.

In the second stage – the measurement stage or update step - a multi-model fusion procedure, similar to the propagation fusion, is performed every mT_M time steps (T_M measurement period, m =1,2,…) employing the additional sensor measurements given in (2). Filter output is the estimated state vector $\hat{\mathbf{x}}_k$. In general any state vector of the estimated sets can be used. Practically the midpoint of one of the estimated set is chosen. Possible is, for example, always to choose the midpoint of the same set or to sort out the set with the minimum volume at every time step. Which procedure exactly should be used, depends on the subsequent applications tasks using these state estimates (e.g. robot trajectory control).

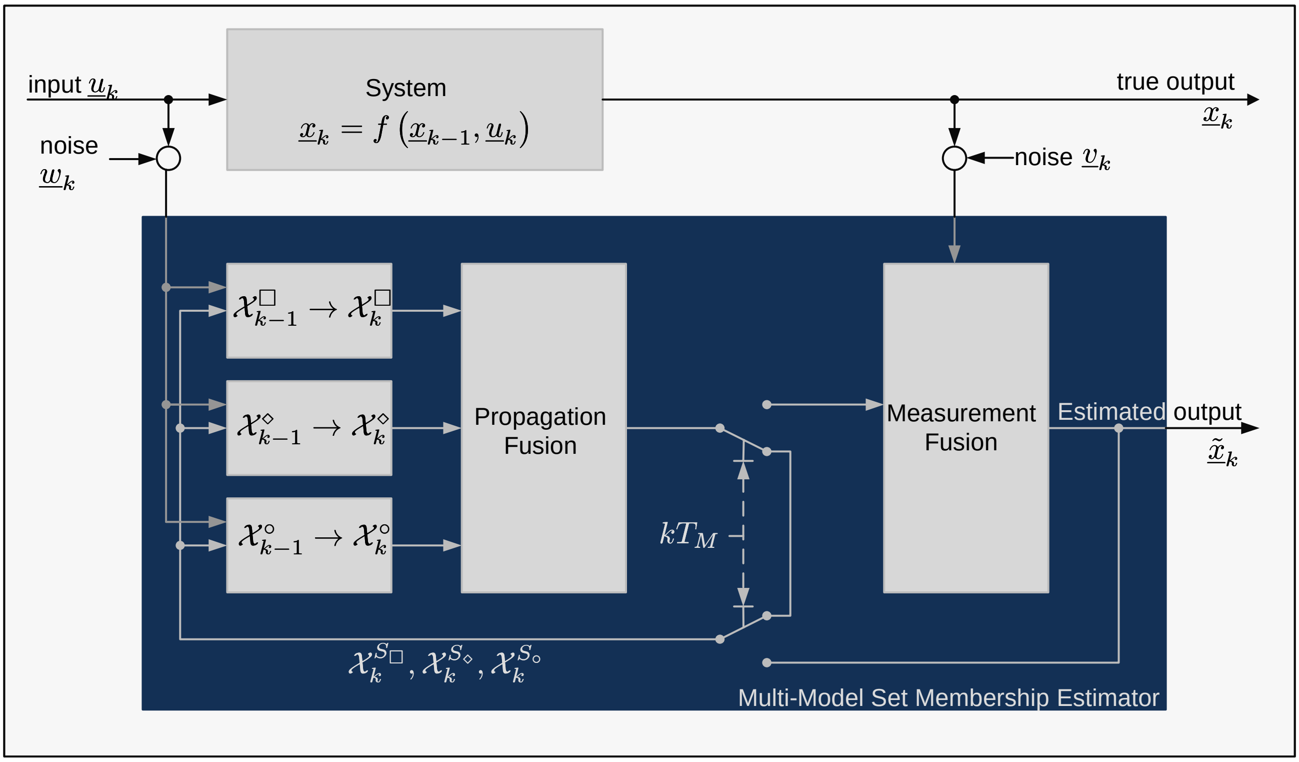

Figure 1: Block diagram of the two stage structure of the introduced multi-model set membership estimator.

Propagation stage. The prediction step is executed within the time interval T_A. Each filter propagates the internal filter states using the linearized system (5), the measured input (3) and the additional input uncertainty $\mathbf{w}_k$ The propagation rules are given by:

- ***Interval set.*** Using the input set $\mathcal{U}_k^{\square} := \underline{\mathbf{u}}_k^{\square} = \mathbf{u}_k^M + \underline{\mathbf{e}}_w$ the predicted interval set $\underline{\mathbf{x}}_k^{\square}$ can be computed via $\mathcal{X}_k^{\square} := \underline{\mathbf{x}}_k^{\square} = \mathbf{A}_k \underline{\mathbf{x}}_{k-1}^{\square} + \mathbf{B}_k \underline{\mathbf{u}}_k^{\square}$.

- ***Ellipsoid set***. For calculating the predicted ellipsoid set $\mathcal{X}_k^{\circ} := \left\{\mathbf{x}_k^{\circ} : \left(\mathbf{x}_k^{\circ} - \breve{\mathbf{x}}_k^{\circ}\right)^T \mathbf{X}_k \left(\mathbf{x}_k^{\circ} - \breve{\mathbf{x}}_k^{\circ}\right)^T \le 1\right\}$ the input interval set $\mathcal{U}_k^{\square}$ has to be circumscribed with an ellipsoid $\mathcal{U}_k^{\circ} := \left\{\mathbf{u}_k^{\circ} : \left(\mathbf{u}_k^{\circ} - \breve{\mathbf{u}}_k^{\circ}\right)^T \mathbf{U}_k \left(\mathbf{u}_k^{\circ} - \breve{\mathbf{u}}_k^{\circ}\right) \le 1\right\}$. Further the midpoint of $\mathcal{X}_k^{\circ}$ can be computed with $\breve{\mathbf{x}}_k^{\circ} = \mathbf{A}_k \breve{\mathbf{x}}_{k-1}^{\circ} + \mathbf{B}_k \breve{\mathbf{u}}_k^{\circ}$.
  For calculating the matrix $\mathbf{X}_k$ the procedure described in (Hanebeck, (1996)) is chosen.

- ***Parallelepiped set.*** To propagate $\mathcal{X}_{k-1}^{\lozenge}$ the input set $\mathcal{U}_k^{\lozenge} = \mathcal{U}_k^{\square}$ can be used. The new parallelepiped set $\mathcal{X}_k^{\lozenge} := \mathbf{T}_k \lozenge \hat{\mathbf{x}}_k^{\lozenge}$ comprises the new interval vector $\underline{\mathbf{x}}_k^{\lozenge} = \left(\mathbf{T}_k^{-1} \mathbf{A}_k \mathbf{T}_{k-1}\right) \underline{\mathbf{x}}_{k-1}^{\lozenge} + \mathbf{T}_k^{-1} \mathbf{B}_k \underline{\mathbf{u}}_k^{\lozenge}$ and the propagated matrix $\mathbf{T}_k = \mathbf{A}_k \mathbf{T}_{k-1}$.
  By using the given formula it is suggested, that the system satisfies the constraint that $\mathbf{T}_k$ stays regular and well-conditioned over the whole time. When this assumption is not true, an additional term for calculating $\mathbf{T}_k$ can be introduced (Lohner, 1988).

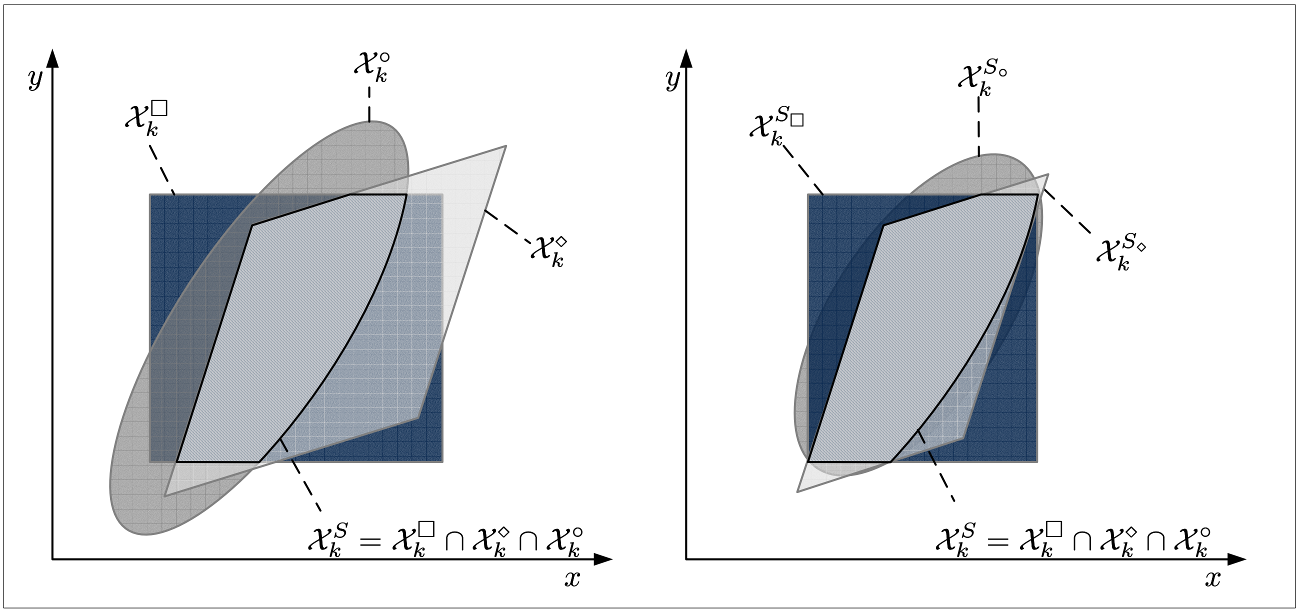

Figure 2: Principle of computing the minimal volume circumscriptions $\mathcal{X}_k^{S_\square}$, $\mathcal{X}_k^{S_\bigcirc}$ and $\mathcal{X}_k^{S_\diamond}$ from the intersection in the two dimensional space. In the left picture the three propagated sets $\mathcal{X}_k^{\square}$, $\mathcal{X}_k^{\bigcirc}$, $\mathcal{X}_k^{\diamond}$ and the resulting intersection $\mathcal{X}_k^{S}$ are displayed. The right picture shows the sets similar to $\mathcal{X}_k^{\square}$, $\mathcal{X}_k^{\bigcirc}$ and $\mathcal{X}_k^{\diamond}$ which circumscribe $\mathcal{X}_k^{S}$ with minimal volume.

After propagating the different sets a fusion takes place with the aim to minimize the volume of the calculated sets. The simplified principle is shown in Figure 2. Here it is not emphasized calculating the proper intersection (8) but rather the circumscription of the minimum volume regions (9) by the respective set descriptions what allows an easy reuse of the fused estimates in a recursive filter scheme. For computing these circumscriptions without calculating the real intersection $\mathcal{X}_k^{S}$ – which could be done by time-consuming numerical methods – only a few simple methods, as listed below, are required:

- **Circumscription of an ellipsoid using a hypercube** $\mathcal{X}^{\square(\bigcirc)}$. $\mathcal{X}^{\square(\bigcirc)} = \left[\mathbf{x}^{\min}, \mathbf{x}^{\max}\right]$, where $\mathbf{x}^{\min}$ represents the vector of minimal extremal values and $\mathbf{x}^{\max}$ the vector of maximal extremal values of the circumscribed ellipsoid $\mathcal{X}^{\bigcirc}$

- **Circumscription of an ellipsoid using a parallelepiped** $\mathcal{X}^{\diamond(\bigcirc)}$. For calculating the parallelepiped $\mathcal{X}^{\diamond(\bigcirc)} = \mathbf{T}\diamond\underline{\mathbf{x}}^{\diamond}$ with the known matrix $\mathbf{T}$, the given ellipsoid $\mathcal{X}^{\bigcirc}$ is transformed with $\mathbf{T}^{-1}$ and circumscribed by a hypercube $\mathcal{X}^{\square_T} = \underline{\mathbf{x}}^{\square}$ around the new ellipsoid $\mathcal{X}^{\bigcirc_T}$. The wanted interval vector $\underline{\mathbf{x}}^{\diamond}$ corresponds with $\underline{\mathbf{x}}^{\square}$.

- **Circumscription of a hypercube using an ellipsoid** $\mathcal{X}^{\bigcirc(\square)}$. The midpoint $\breve{\mathbf{x}}^{\bigcirc}$ of the wanted ellipsoid $\mathcal{X}^{\bigcirc(\square)} := \left\{\mathbf{x}^{\bigcirc} : \left(\mathbf{x}^{\bigcirc} - \breve{\mathbf{x}}^{\bigcirc}\right)^T \mathbf{X}\left(\mathbf{x}^{\bigcirc} - \breve{\mathbf{x}}^{\bigcirc}\right)^T \leq 1\right\}$ corresponds with the midpoint of the hypercube $\breve{\mathbf{x}}^{\square} = \dfrac{\mathbf{x}^{-} + \mathbf{x}^{+}}{2}$. The diagonal matrix $\mathbf{X}$ can be computed via $\mathbf{X} = \operatorname{diag}\left(\dfrac{4}{n\left(\mathbf{x}^{+} - \mathbf{x}^{-}\right)^2}\right)$.

- **Circumscription of a parallelepiped using an ellipsoid** $\mathcal{X}^{\bigcirc(\diamond)}$. To circumscribe the parallelepiped $\mathcal{X}^{\diamond} = \mathbf{T}\diamond\underline{\mathbf{x}}^{\diamond}$ with an ellipsoid $\mathcal{X}^{\bigcirc(\diamond)}$, simply $\underline{\mathbf{x}}^{\diamond}$ can be circumscribed by an ellipsoid $\mathcal{X}^{\bigcirc(\square)}$ using the methods described above. The midpoint of $\mathcal{X}^{\bigcirc(\diamond)}$ can then be computed with $\breve{\mathbf{x}}^{\bigcirc(\diamond)} = \mathbf{T}\breve{\mathbf{x}}^{\bigcirc(\square)}$ and the matrix computed with $\mathbf{X}^{\bigcirc(\diamond)} = \mathbf{T}^{-T}\mathbf{X}^{\bigcirc(\square)}\mathbf{T}^{-1}$.

- **Circumscription of a parallelepiped using a hypercube $\mathcal{X}^{\square(\lozenge)}$.** The minimal bounding hypercube of a parallelepiped can be found by examination of the vector of its edges $\mathbf{P}$ and is given as $\underline{\mathbf{x}}^{\square(\lozenge)} = \left[\min(\mathbf{P}), \max(\mathbf{P})\right]$.

- **Circumscription of a hypercube using a parallelepiped $\mathcal{X}^{\lozenge(\square)}$.** For calculating $\mathcal{X}^{\lozenge(\square)} = \mathbf{T}\lozenge\underline{\mathbf{x}}^{\lozenge}$ with the given matrix $\mathbf{T}$, the hypercube $\mathcal{X}^{\square} = \underline{\mathbf{x}}^{\square}$ can be first transformed with $\mathbf{T}^{-1}$ and the resulting parallelepiped $\mathcal{X}^{\lozenge^*(\square)} = \mathbf{T}^{-1}\lozenge\underline{\mathbf{x}}^{\square}$ can be circumscribed with a hypercube $\mathcal{X}^{\square^*(\lozenge)} = \underline{\mathbf{x}}^{\square^*(\lozenge)}$ as described above. The wanted parallelepiped can now be computed via $\mathcal{X}^{\lozenge(\square)} = \mathbf{T}\lozenge\underline{\mathbf{x}}^{\square^*(\lozenge)}$.

Propagation Fusion. Having calculated the circumscriptions and assuming that the true state $\mathbf{x}_k$ is element of each three estimated sets ($\mathcal{X}_k^S = \mathcal{X}_k^{\square} \cap \mathcal{X}_k^{\bigcirc} \cap \mathcal{X}_k^{\lozenge} \neq \emptyset$) it is straightforward to intersect the existing hypercubes $\mathcal{X}_k^{\square(\bigcirc)}$, $\mathcal{X}_k^{\square(\lozenge)}$, $\mathcal{X}_k^{\square}$, the parallelepipeds $\mathcal{X}_k^{\lozenge(\bigcirc)}$, $\mathcal{X}_k^{\lozenge(\square)}$, $\mathcal{X}_k^{\lozenge}$ and the ellipsoids $\mathcal{X}_k^{\bigcirc(\square)}$, $\mathcal{X}_k^{\bigcirc(\lozenge)}$, $\mathcal{X}_k^{\bigcirc}$ by using the methods given in section 3. As a result the convex sets $\mathcal{X}_k^{S_\square}$, $\mathcal{X}_k^{S_\bigcirc}$ and $\mathcal{X}_k^{S_\lozenge}$ circumscribe the real intersection area with minimal volume.

Measurement Fusion. During the time step $mT_M = kT_A$, when an observation of the system via an uncertain output measurement is available, an estimation update step will be executed. Here the employed procedure is similar to the intersection method used in the propagation stage – except that here the circumscriptions $\mathcal{X}_k^{M_\square}$, $\mathcal{X}_k^{M_\bigcirc}$ and $\mathcal{X}_k^{M_\lozenge}$ of the available measurement are added to the intersected sets, which were calculated during the propagation stage. Especially during longer estimation periods this stage ensures a reasonable bounded volume of the calculated sets.

5. Localization of a mobile robot via multi-model set membership estimator

The functionality and performance of the introduced filter shall be demonstrated by an example of localization of a mobile robot in a flat environment. In the next paragraphs the results of the accomplished simulations are reported. The described system refers to a real existing platform on which the testing of the proposed algorithms is in progress as well.

System description. It is assumed that the differential-drive robot shown in Figure 3 is moving in a flat environment, which can be adequately described by a two-dimensional reference frame x and y. The orientation of the vehicle with respect to the reference frame is given by φ. The robot is equipped with additional odometers, which provide measurements of the robot displacement $\hat{\mathbf{x}}_k^{\Delta} = \mathbf{x}_k^{\Delta} + \mathbf{w}_k$ during a sampling period T_A. Under the assumption of slow dynamics, the motion of the robot can be approximately expressed by the simplified time discrete kinematic model

$$\mathbf{x}_k = \begin{pmatrix} x_k \\ y_k \\ \varphi_k \end{pmatrix} = \mathbf{x}_{k-1} + \underbrace{\begin{bmatrix} \cos(\varphi_{k-1}) & -\sin(\varphi_{k-1}) & 0 \\ \sin(\varphi_{k-1}) & \cos(\varphi_{k-1}) & 0 \\ 0 & 0 & 1 \end{bmatrix}}_{\mathbf{H}_k} \mathbf{x}_k^{\Delta}. \tag{10}$$

Further on it is considered that the robot has the ability to measure its own pose globally within certain error bounds $\underline{\mathbf{e}}_v$.

To estimate the pose of the robot with help of the introduced estimation filter, the system model (10) is linearized at the midpoint of the sets $\breve{\mathbf{x}}$, which results the linear time variant state space model

$$(\hat{\mathbf{x}}_k - \breve{\mathbf{x}}_k) = \underbrace{\begin{pmatrix} 1 & 0 & -(\breve{y}_k - \breve{y}_{k-1}) \\ 0 & 1 & (\breve{x}_k - \breve{x}_{k-1}) \\ 0 & 0 & 1 \end{pmatrix}}_{\mathbf{A}_k} (\hat{\mathbf{x}}_{k-1} - \breve{\mathbf{x}}_{k-1}) + \underbrace{\begin{pmatrix} \cos(\breve{\varphi}_{k-1}) & -\sin(\breve{\varphi}_{k-1}) & 0 \\ \sin(\breve{\varphi}_{k-1}) & \cos(\breve{\varphi}_{k-1}) & 0 \\ 0 & 0 & 1 \end{pmatrix}}_{\mathbf{B}_k} (\hat{\mathbf{x}}_k^{\Delta} - \breve{\mathbf{x}}_k^{\Delta}). \tag{11}$$

With the given system the measurement equation results to

$$\mathbf{x}_k^M = \mathbf{x}_k + \mathbf{v}_k. \tag{12}$$

In the case of employing set estimates it is not necessary to determine the specific distribution function of the used localization sensor system as long as it can presumed to be bounded.

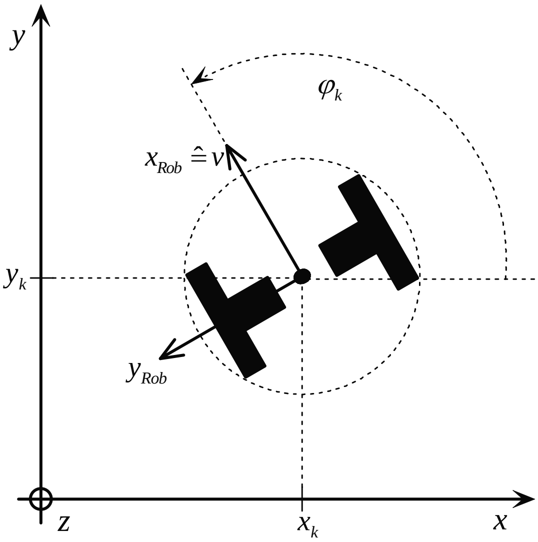

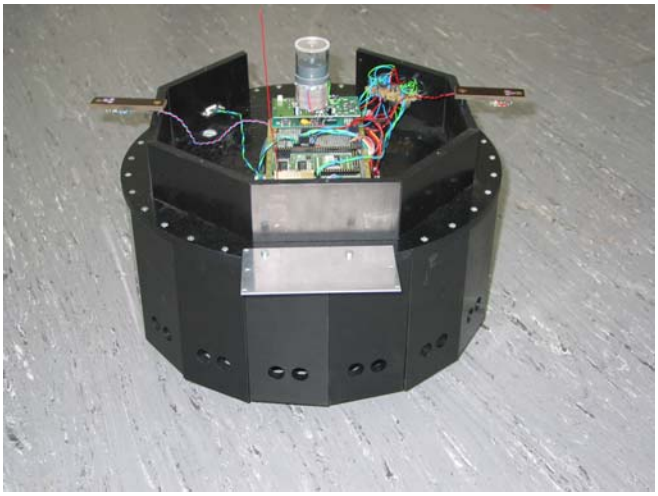

Figure 3: Reference frame of the used differential-drive mobile robot (left) and a picture of the original robot MP2 (right)

Accomplished experiments. To determine the properties of the proposed filter a simulation in Matlab/Simulink was implemented. The relevant experiment parameters are shown in Table 1. Please note that the experiment time history diagrams shown below do not have the same scaling.

Table 1: Simulation parameters

t_0	[s]	0	v	[m/s]	0.3	$\breve{\mathbf{x}}_0$	$(2.1\,\text{m}, \quad 2.3\,\text{m}, \quad 0°)^T$
t_{end}	[s]	150	w	[1/s]	0.5	$\underline{\mathbf{e}}_w$	$\pm(0.25\,\text{mm}, \quad 0.25\,\text{mm}, \quad 0.0015°)^T$
T_A	[s]	1				$\underline{\mathbf{e}}_v$	$\pm(15\,\text{cm}, \quad 15\,\text{cm}, \quad 3°)^T$

At first the performances of the three stand-alone set based filters (interval set filter, parallelepiped set filter, ellipsoid set filter) were examined. For this purpose three different trajectories have been simulated:

1. Trajectory quadrangle with an edge length of ten metres
2. Trajecory circle with a radius of five metres
3. Trajectory turning (Robot turns at its place.).

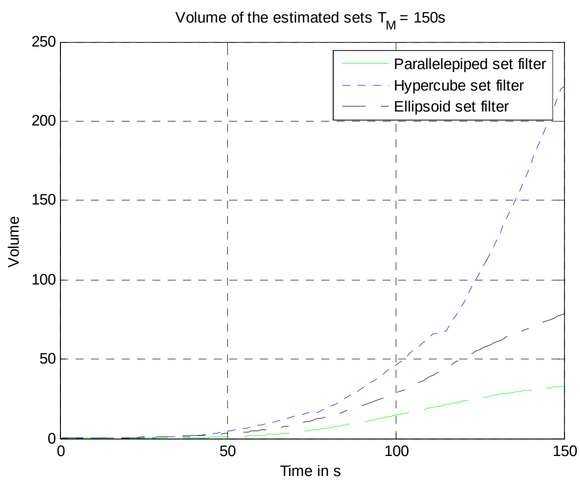

Figure 4a: Trajectory quadrangle – pure propagation: Comparison of the volume of the estimated sets using the stand-alone set based filters (interval set filter, parallelepiped set filter, ellipsoid set filter)

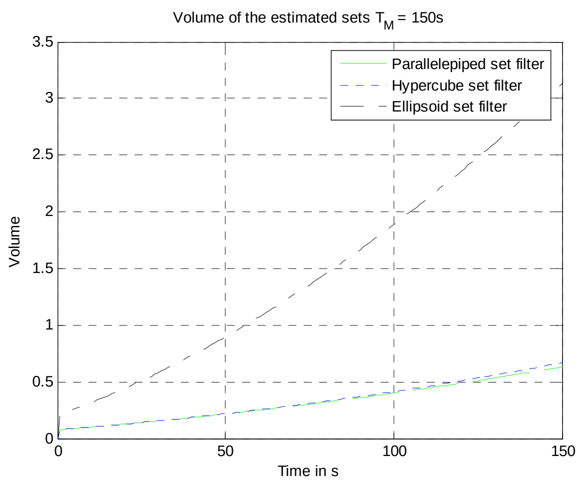

Figure 4b: Trajectory turning – pure propagation: Comparison of the volume of the estimated sets using the stand-alone set based filters (interval set filter, parallelepiped set filter, ellipsoid set filter)

The results of the simulation experiments for pure propagation without additional measurement are shown in Figure 4. As you can easily see, behave the described set based filters different depending on the trajectory. Using the quadrangle (Figure 4a) the filter based on the parallelepiped set estimates the state sets with the least volume and the hypercube set filter gives states with very big uncertainty bound. These circumstances change by turning the robot on a spot (Figure 4b). The filters based on hypercube or parallelepiped can narrow the uncertainty as the ellipsoid set filter shows a bad estimation quality.

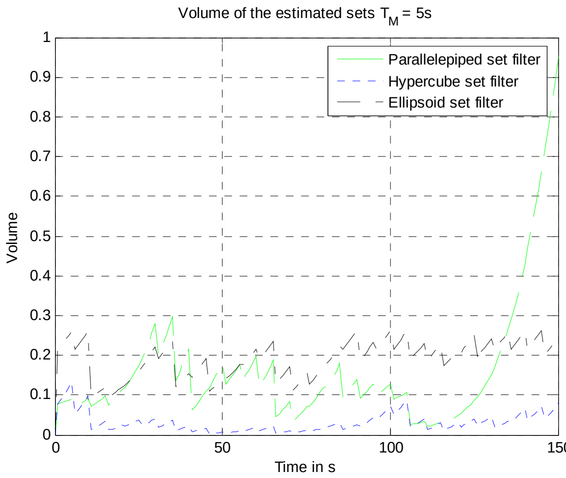

Figure 5a: Trajectory circle – propagation & measurement: Comparison of the volume of the estimated sets using the stand-alone set based filters (interval set filter, parallelepiped set filter, ellipsoid set filter) with a measurement step of $T_M = 5$s

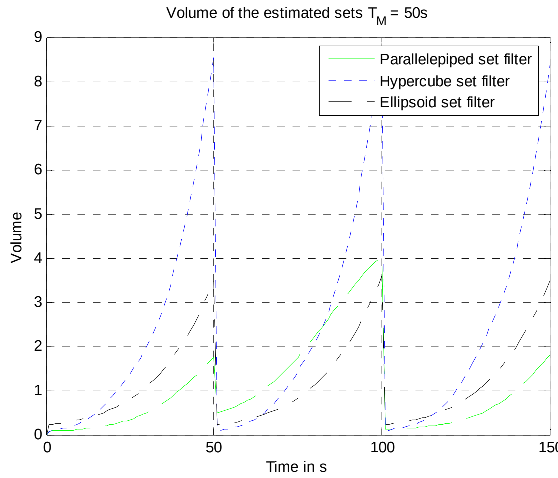

Figure 5b: Trajectory circle – propagation & measurement: Comparison of the volume of the estimated sets using the stand-alone set based filters (interval set filter, parallelepiped set filter, ellipsoid set filter) with a measurement step of $T_M = 100$s

A similar fact can be shown by comparing simulation runs with varied measurement step T_M as done in (see Figure 5a/b and Figure 6a).

If T_M is very small, the hypercube set filter can benefit most from the measurement carried out as with larger breaks between the measurements the filters based on the ellipsoid set and on the parallelepiped set respectively brings the better results.

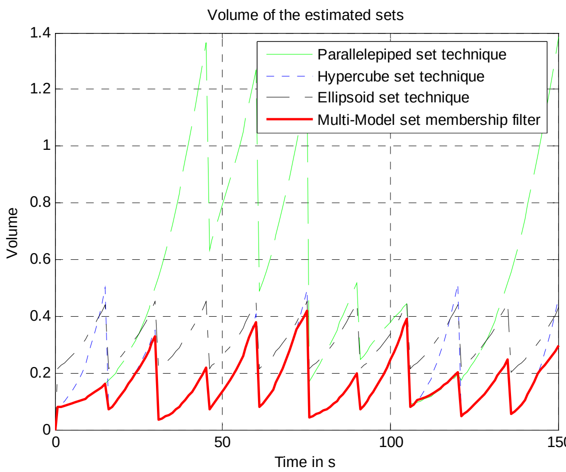

Figure 6a: Trajectory circle – multi-model estimator: Comparison of the volume of the estimated sets using the set based filters themselves (interval set filter, parallelepiped set filter, ellipsoid set filter) and the multi-model set membership filter (solid line) with a measurement step of $T_M = 15$s

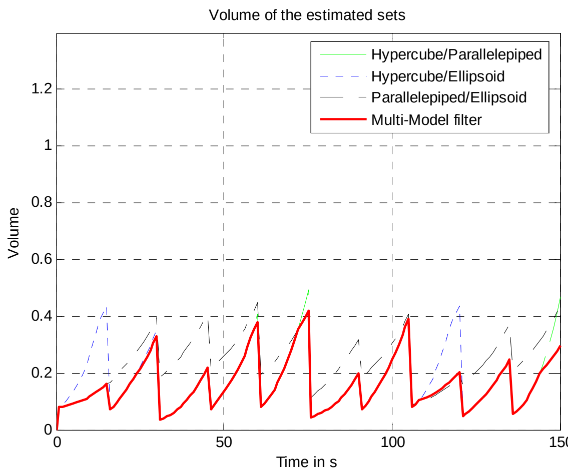

Figure 6b: Trajectory circle – reduced multi-model estimator: Comparison of the volume of the estimated sets using the set based filters consisting of two set based techniques (hypercube/ellipsoid set, hypercube/parallelepiped set, parallelepiped/ellipsoid set) and the multi-model set membership filter (solid line) with a measurement step of $T_M = 15$s

To reach an optimal estimation independent of system parameters the multi-model set membership estimation filter has been implemented. A comparison between the introduced filter and the three established filters is shown in Figure 6a. Here the minimal volume of the multi-model set membership estimation filter $V^{\min} = \min(V^{\square}, V^{\Diamond}, V^{\bigcirc})$ is plotted against the volume the filter based on interval set technique, parallelepiped set technique and ellipsoid set technique respectively. As can be seen easily the multi-model filter behaves best and computes the set with minimal volume. In Figure 6b the multi-model filter has been confronted with reduced filters based on the combination of each with two set methods. Still the multi-model filter reaches the best result, but for applications where calculation time is valuable, a reduced filter can perform satisfactory as well (see Figure 7 for comparing the relative calculation time of the implemented filters). In such a case the filter, which fits best, should be chosen considering the underlying system parameters.

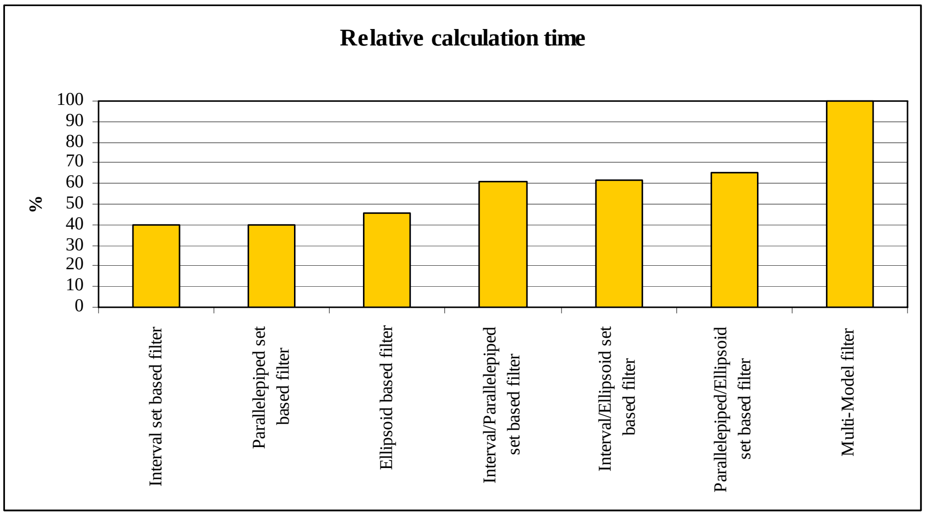

Figure 7: Comparison of the relative calculation time of the different implemented set estimation filters

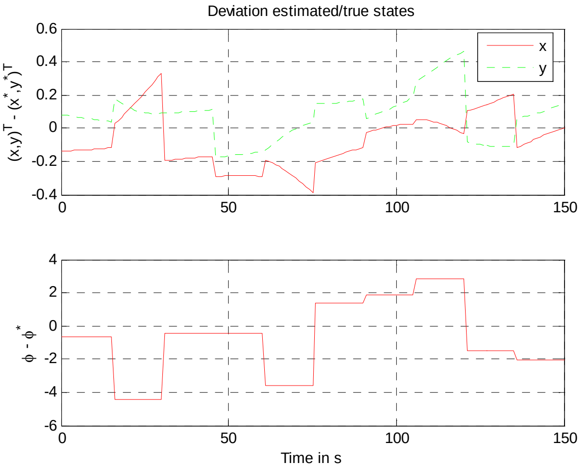

Figure 8: Example for the trend of the deviation between true state and estimated state (Trajectory = circle / $T_M = 15\text{s}$)

For applications where system parameters can change quickly – as the trajectory or the measurement frequency does in mobile robotics – implementing the proposed multi-model filter seems quite reasonable. For navigation purposes a specific estimated pose out of the set of possible poses has to be selected. Extracting the midpoint $\breve{\mathbf{x}}_k^{\min}$ of the set with the minimal volume $\mathcal{X}_k^*\left(V^{\min}\right)$, $* \in \{\square, \bigcirc, \Diamond\}$ may be one solution. Figure 8 shows an example for the deviation $\mathbf{x}_k - \breve{\mathbf{x}}_k^{\min}$. The mean estimation error of the distance between the estimated pose and the true pose of the robot is 0.12 m and a standard deviation 0.08 m. The estimation error of the orientation reaches a mean of 1,9° and a standard deviation of 1,2°.

6. Conclusions

Tasks of controlling or navigation require always estimating internal system states, which are not directly observable or only known with some uncertainty. If a stochastic description of the uncertainty is available an extended or unscented Kalman filter can be applied. But in many cases the required system properties can only be examined with big effort, if at all. A more general approach is to describe uncertainties with the help of set theoretic models, which describe an uncertainty using its bounding geometrical properties. Thus the underlying properties do not have to be known, but must be considered only as bounded. Established methods for set theoretic descriptions can be found in literature for compact and convex structures like boxes, parallelepipeds and ellipsoids. In opposite to the stochastic implementations set theoretic approaches result in more or less conservative over approximations depending on the system properties and the actual system parameters. Considerable sensitivity of localization behaviour for a differential-drive robot could be shown just by changing the trajectory of the robot and the measurement interval. According to this and with the aim to reach a robust and optimal estimation independent of changing system parameters a new multi-model estimator consisting of the named set theoretic descriptions has been introduced and examined within this paper. In comparison to the established methods and independent from the instantaneous parameters the volume of the set of estimated states could be reduced and an adequate estimation performance was reached.

A next challenging problem – already in progress – is the implementation of the filter on an existing mobile robot platform and developing a compatible trajectory control strategy, which makes best use of the strengths of the developed filter. Further a more precisely examination of the convergence behaviour of the multi-model set membership filter will bring reliable prognoses about the stability and performance of the filter.

References

Alefeld G. and J. Herzberger (1983). *Introduction to Interval Computations*. Academic Press, New York.

Cox I.J. (1991). Blanche – an experiment in guidance and navigation of an autonomous robot vehicle. *IEEE Transactions on Robotics and Automation*. **Vol. 7**, pp:193-204.

Di Marco M., A. Garulli, A. Giannitrapani and A. Vicino (2003). Simultaneous localization and map building for a team of cooperating robots: a set membership approach. *IEEE Transactions on Robotics and Automation*. **Vol. 19-2**, pp: 238-249.

Garulli A. and A. Vicino (2001). Set membership localization of mobile robots via angle measurement. *IEEE Transactions on Robotics and Automation*. **Vol. 17-4**, pp: 450-463.

Hanebeck U.D. (1996). *Lokalisierung eines mobilen Roboters mittels effizienter Auswertung von Sensordaten und mengenbasierter Zustandsschätzung*. PhD thesis. Technische Universität München, Germany

Hanebeck U.D. and G. Schmidt (1997). Mobile robot localization based on efficient processing of sensor data and set theoretic estimation. In: *Proceedings of the Fifth International Symposium on Experimental Robotics (ISER'97)*. pp: 321-332. Barcelona, Spain.

Hanebeck U.D. and J. Horn (2000). Fusing Information Simultaneously Corrupted by Uncertainties with Known Bounds and Random Noise with Known Distribution. *Information Fusion.* **Vol. 1-1**, pp: 55-63. Elsevier Science.

Horn S. (2003). *Anwendung mengenbasierter Schätzverfahren zur Lokalisierung von mobilen Plattformen in ebenen Umgebungen*. Diplomarbeit (Master Thesis), Technische Universität Dresden, Germany.

Leonard J.J. and H.F. Durrant-Whyte (1991). Mobile robot localization by tracking geometric beacons. *IEEE Transactions on Robotics and Automation*. **Vol. 7**, pp: 376-382.

Lohner R. (1988). *Einschließung der Lösung gewöhnlicher Anfangs- und Randwertaufgaben und Anwendungen*. PhD Thesis. Universität Karlsruhe

Ros L., A. Sabater and F. Thomas (2002). An ellipsoidal calculus based on propagation and fusion. *IEEE Transactions on Systems, Man and Cybernetics – Part B: Cybernetics*. **Vol. 32**, pp: 430-442.

Schweppe F.C. (1968). Recursive state estimation: Unknown but bounded errors and system inputs. *IEEE Transactions on Automatic Control*. **Vol. AC-13/1**, pp: 22-28.

Thrun S. (1993). Exploration and model building in mobile robot domains. In E. Ruspini (ed.): *Proceedings of the IEEE International Conference on Neural Networks*. pp: 175-180. San Francisco, USA

Vicino G. and G. Zappa (1996). Sequential approximation of feasible parameter sets for identification with set membership uncertainty. *IEEE Transactions on Automatic Control*. **Vol. 41-6**, pp: 774-785.

Curriculum vitae of authors

Dipl.-Ing. Sylvia Horn
Dipl.-Ing. degree in electrical engineering (2003) from Technische Universität Dresden, Germany. Since 2003 staff member and Ph.D. student at the Institute of Automation, Technische Universität Dresden, Germany. Research areas: data fusion and mobile robotics

Prof. Dr. techn. Klaus Janschek
Dipl.-Ing. degree in electrical engineering (1979) and Dr.techn. degree (1982) from Technical University Graz, Austria. Industrial affiliations: 1982-1985 Carl Schenck AG, Darmstadt Germany, servohydraulics control system development; 1985-1995 Daimler-Benz Aerospace - Dasa (former MBB - Messerschmitt-Bölkow-Blohm), Munich, Germany, design and development of Guidance, Navigation and Control (GNC) systems for space vehicles and satellites. Since 1995 Full Professor of Automation Engineering with the Technische Universität Dresden, Germany; 2005 Visiting Professor at Stanford University, USA, Aeronautics & Astronautics Department. IPC-Chair IFAC Mechatronics 2006. Research interests: visual navigation, data fusion, mobile robotics, optical data processing and opto-mechatronics.